All-Fibre Comb Filter with Narrow Bandwidth Based on a Dual-Pass Mach-Zehnder Interferometer

Li Wei
Department of Physics and Computer Science, Wilfrid Laurier University, Waterloo, Ontario, Canada

Keywords: Comb Filter, Mach-Zehnder Interferometer, Fibre Loop Mirror, Tunable, Narrow Bandwidth.

Abstract: A theoretical analysis of an all-fibre comb filter with narrow bandwidth is presented, based on a dual-pass Mach-Zehnder interferometer (DP-MZI) with two variable ratio couplers. While the DP-MZI has previously been used to construct a flattop comb filter via the reflection port, in this work it is employed as a narrow bandwidth comb filter through the transmission port. Two conditions are newly derived to determine how to choose the coupling ratios to optimize the optical performance of the proposed comb filter. First, to obtain a lossless narrow-bandwidth filter, the coupling ratios of the two couplers must be equal. Second, to achieve maximum extinction ratio, these coupling ratios are equal to 0.146 or 0.854. The impact of the coupling ratios on bandwidth and extinction ratio is investigated. It is shown that the 3-dB bandwidth can be further reduced by tuning the coupler ratios near the optimal value. This unique property is highly desirable for applications in fibre lasers, optical sensing technology and reconfigurable optical systems.

1 INTRODUCTION

All-fibre comb filters are essential components for processing optical signals in wavelength domain. They have been widely used in dense wavelength-division multiplexed (DWDM) systems, multi-wavelength lasers, and fibre sensor systems due to their low insertion loss, low cost, simple structure, ease of use and fibre compatibility. Various techniques have been employed to construct all-fibre comb filters, including chirped fibre Bragg gratings (Chen, 2024), an acousto-optic coreless fibre core mode blocker (Ramírez-Meléndez, 2017), multimode interference (Zhou, 2018), polarization-diversity loop configurations (Jung, 2017, 2024), fibre-based Lyot filter (Zhu, 2020), fibre-based Mach-Zehnder interferometer (MZI) (Han, 2018), high-birefringent fibre loop mirror (Wei, 2021), hybrid Fabry-Perot/Mach-Zehnder interferometer (Han, 2020), and all-fibre mode selective MZI (Liu, 2021). Much effort has been focused on developing all-fibre comb filters with reconfigurable free-spectral-range (FSR), and tunable wavelength.

On the other hand, the flexibility to control and adjust the bandwidth of the passband and extinction ratio of a comb filter is critical for applications in reconfigurable fibre optical systems (Cheng, 2024), and fibre lasers (Marrujo-García, 2021). Liu et *al*. (Liu, 2024) recently presented a narrow passband bandwidth-tunable comb filter based on silicon rings. Jiang et *al*. demonstrated a wavelength- and bandwidth-tunable silicon comb filter (Jiang, 2016). Although research has been predominantly focused on silicon planar structure, little work has been reported on manipulating the bandwidth of all-fibre comb filters.

In this work, we present an all-fibre comb filter with adjustable bandwidth based on a dual-pass MZI (DP-MZI) configuration with ratio-variable fused fibre couplers. The DP-MZI has been previously employed to construct a multifunctional comb filter [Luo, 2012], and our group has demonstrated a continuously tunable flattop comb filter based on this configuration [Wei, 2019], both of which have used the reflection port as the output. In this work, however, the transmission port is employed to achieve a narrow bandwidth at passband by taking advantage of the flattop condition at resonance. The optimum condition for achieving a lossless comb filter is derived along with the condition for maximizing the extinction ratio. It is also found that the bandwidth of the comb filter can be tuned by adjusting the coupling ratios.

Wei, L.
All-Fibre Comb Filter with Narrow Bandwidth Based on a Dual-Pass Mach-Zehnder Interferometer.
DOI: 10.5220/0013144300003902

In *Proceedings of the 13th International Conference on Photonics, Optics and Laser Technology (PHOTOPTICS 2025)*, pages 87-91
ISBN: 978-989-758-736-8; ISSN: 2184-4364

2 OPERATION PRINCIPLE

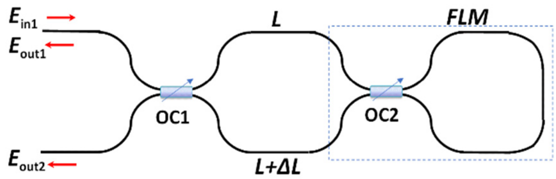

Figure 1: Schematic diagram of the proposed comb filter.

Figure 1 shows the schematic diagram of the proposed comb filter constructed with two coupling-ratio variable couplers (OC1 and OC2). Assume that couplers and fibres are polarization independent. The path difference between the two arms of the OC1 and OC2 is ΔL. The two right ends of the OC2 are spliced to form a fibre loop mirror (FLM). It is well known that a FLM with a 3-dB coupler is a 100% reflector. If OC2 is a 3-dB coupler, the two beams at top- and bottom-arm will reflect along the same path. As a result, the comb filter formed by two 3-dB couplers acts as a regular MZI with the path difference of the two interference beams being $2\Delta L$. When the coupling ratio of the OC2 is not equal to 50%, both top- and bottom-beams will be partially reflected via the same path and partially transmitted to the bottom and top paths, respectively, creating multiple interference beams, with path differences being ΔL and $2\Delta L$. The output functions at reflective and transmissive ports can be written as (Luo, 2012):

$$\begin{aligned} R_{port1} &= 4c_1^2c_2(1-c_2)+4c_2(1-c_1)^2(1-c_2)+4c_1(1-c_1)(1-2c_2)^2 \\ &+8(1-2c_1)(1-2c_2)\sqrt{c_1c_2(1-c_1)(1-c_2)}\cos\phi \\ &-8c_1c_2(1-c_1)(1-c_2)\cos 2\phi, \end{aligned} \tag{1}$$

$$\begin{aligned} T_{port2} &= 8c_1c_2(1-c_1)(1-c_2)+(1-2c_1)^2(1-2c_2)^2 \\ &-8(1-2c_1)(1-2c_2)\sqrt{c_1c_2(1-c_1)(1-c_2)}\cos\phi \\ &+8c_1c_2(1-c_1)(1-c_2)\cos 2\phi, \end{aligned} \tag{2}$$

where c_1 and c_2 are the coupling ratios of OC1 and OC2, and $\phi = n\Delta L/\lambda$ is the phase shift between two interference beams, n is the refractive index of the optical fibre, and λ is the operation wavelength. The output includes periodic terms ($\cos\phi$ and $\cos 2\phi$) with opposite sign, contributed from single- and dual-pass interference beams. The FSR of the dual-pass term is half that of the single-pass term. A weak contribution from dual pass may give rise to a flattop response at port 1 with twice the FSR of the regular MZI mentioned above. Note that the proposed filter is a polarization independent filter.

With properly choosing the coupling ratios of the two couplers, a flattop spectrum at reflection (output port1) can be achieved from our previous study (Wei, 2019):

$$\begin{aligned} &4c_1^2c_2(1-c_2)+4c_2(1-c_1)^2(1-c_2)+4c_1(1-c_1)(1-2c_2)^2 \\ &+8(1-2c_1)(1-2c_2)\sqrt{c_1c_2(1-c_1)(1-c_2)} \\ &-8c_1c_2(1-c_1)(1-c_2)=1, \end{aligned} \tag{3}$$

where Eq. (3) is obtained by setting the reflectance (at port 1) to be unit, i.e., $R=1$ at the resonance condition.

The equation above is equivalent to the condition by setting the transmission (at port 2) to be zero at resonance, i.e., $T=0$ as follows:

$$\begin{aligned} &8c_1c_2(1-c_1)(1-c_2)+(1-2c_1)^2(1-2c_2)^2 \\ &-8(1-2c_1)(1-2c_2)\sqrt{c_1c_2(1-c_1)(1-c_2)} \\ &+8c_1c_2(1-c_1)(1-c_2)=0. \end{aligned} \tag{4}$$

The flattop condition in Eq. (4) can be further simplified:

$$1-4c_1(1-c_1)-4c_2(1-c_2)=0. \tag{5}$$

Eq. (5) will be used to find the optimal value of the coupling ratio for maximizing the extinction ratio. Additionally, Eq. (5) can be solved as:

$$c_2 = \frac{1}{2}\left(1 \pm 2\sqrt{c_1(1-c_1)}\right). \tag{6}$$

Eq. (6) agrees with the simulated results from our previous study (Wei, 2019).

While the passband spectrum of the comb filter at port 1 for reflection can be flattened with increased bandwidth at resonance, the bandwidth of the comb filter at port 2 for transmission can be significantly narrowed at anti-resonance. This unique property can be utilized in designing narrow-bandwidth comb filter by using port 2 as output.

To obtain a lossless narrow-bandwidth spectral response, the transmission of the comb filter at port 2 must have a unit magnitude at anti-resonance (i.e., $\phi = p\pi$, where p is an odd integer), which gives the following condition:

$$\begin{aligned} &8c_1c_2(1-c_1)(1-c_2)+(1-2c_1)^2(1-2c_2)^2 \\ &+8(1-2c_1)(1-2c_2)\sqrt{c_1c_2(1-c_1)(1-c_2)} \\ &+8c_1c_2(1-c_1)(1-c_2)=1. \end{aligned} \tag{7}$$

By solving Eq. (7), the solution is found to be:

$$c_1 = c_2. \tag{8}$$

Therefore, the optimum condition for a lossless narrow-bandwidth comb filter is that the two couplers must have identical coupling ratios.

Note that Eq. (8) represents the lossless condition, i.e., the zero insertion condition. On the other hand, high extinction is desirable to effectively isolate noise in the stopband. To achieve maximum extinction ratio, the transmission at the stopband must be zero, which corresponds to the flattop condition in Eq. (5) at resonance for a flattop comb filter. By solving Eq. (5) and Eq. (8), we can find the solution to achieve maximum extinction ratio for a narrow bandwidth is:

$$c_1 = c_2 = \frac{2 \pm \sqrt{2}}{4}. \quad (9)$$

This indicates that the coupling ratios of the two couplers are equal and can be either 0.146, or 0.854.

In Section 3, we will present simulated results of the proposed narrow bandwidth comb filter, and characterize the impact of the coupling ratios to the bandwidth and extinction ratio of the transmissive comb filter.

3 NUMERICAL RESULTS

Figure 2 shows the narrow bandwidth spectra of the proposed comb filter for three different coupling ratios where $c_1 = c_2$. It is evident that the peaks of the three curves overlap at unit for different coupling ratios, indicating that the comb filter remains lossless as long as the two couplers have the equal coupling ratios. The red curve with $c_1 = c_2 = 0.146$, represents the optimized solution in Eq. (9), demonstrating that zero transmission at stopband with a flattop shape, indicating the extinction ratio reaches its maximum. When the coupling ratio deviates from the optimal value, the transmission at stopband increases, suggesting a degradation in the extinction ratio. For the coupling ratios smaller or larger than the optimal value (as shown in the green and blue curves), the bandwidth increases or decreases, respectively.

To clearly illustrate the impact of varying the coupling ratio with $c_1 = c_2$, Fig. 3 plots the 3-dB bandwidth and the extinction ratio as the coupling ratio varies from 0.106 to 0.186. The FSR of the comb filter is 0.82 nm. At the optimal coupling ratio (0.146), the extinction ratio reaches its maximum and the 3-dB bandwidth is 0.298 nm. For comparison, the 3-dB bandwidth of a standard MZI is half of the FSR, i.e., 0.41 nm. The means the 3-dB bandwidth of the proposed comb filter is 27.3% narrower than that of the standard MZI.

Furthermore, as the coupling ratio increases the 3-dB linewidth decreases, suggesting that the bandwidth of the comb filter can be further narrowed by increasing the coupling ratio, though at the expense of the extinction ratio.

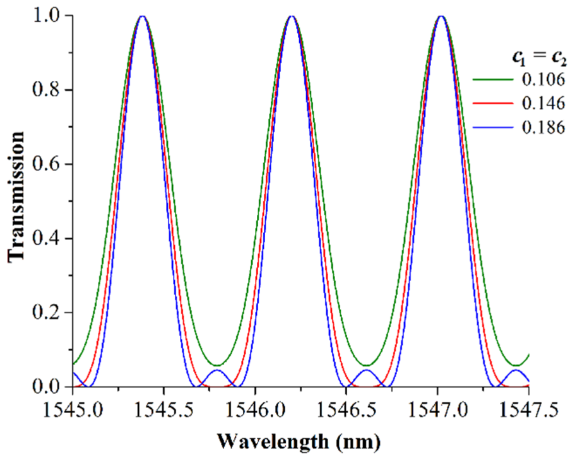

Figure 2: The spectra of the proposed comb filter for different coupling ratios with $c_1 = c_2$.

Note that in Fig. 3, the same coupling ratio is used for both couplers. It would be very insightful to explore how the key specifications change when the coupling ratios c_1 and c_2 are different.

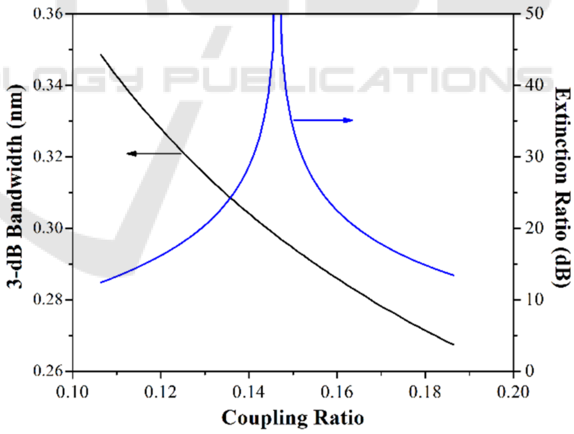

Figure 3: The 3-dB bandwidth and extinction ratio as a function of the coupling ratio with $c_1 = c_2$.

Fig. 4(a) show the performance of the 3-dB bandwidth for three fixed values of c_1, while c_2 varies. For a fixed coupling ratio c_1, the 3-dB bandwidth decreases as c_2 increases. Additionally, increasing the fixed coupling ratio c_1 results in a narrower 3-dB bandwidth.

Fig. 4(b) displays the extinction ratio as a function of c_2 for three fixed values of c_1. When c_1 is set to be the optimal value (see the red line), the curve shows near symmetry at $c_1 = c_2$; however, when c_2 deviates from the optimal value, the extinction ratio degrades. When c_1 is smaller than the optimal value (as shown by the grey line), the extinction ratio increases with c_2. Conversely, when c_1 is larger than the optimal value, the extinction ratio (as shown in blue line) decreases as c_2 increases.

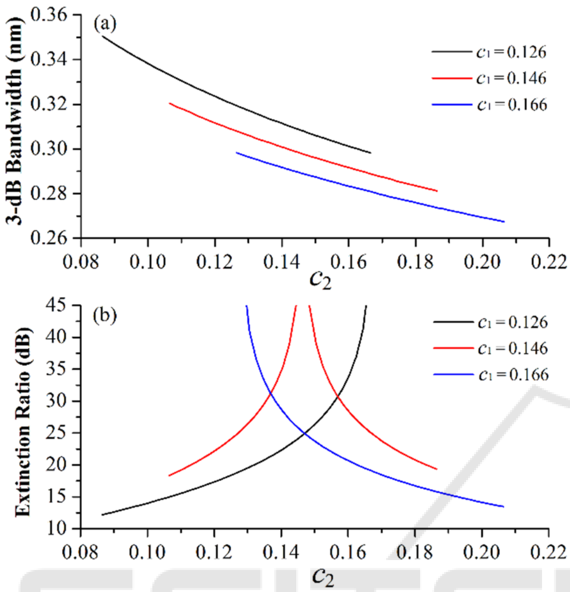

Fig.4: (a) The 3-dB bandwidth and (b) extinction ratio as a function of c_2 with different fixed c_1.

Thus, both the 3-dB bandwidth and extinction ratio can be dynamically tuned with adjusting the two coupling ratios. As shown in Fig. 4, desirable optical performance can also be achieved by suitable choosing the combination of c_1 and c_2. To obtain a narrow bandwidth with a high extinction ratio, if c_1 is smaller than the optimal value, then c_2 must be greater than the optimal value, and similarly, if c_2 is larger than the optimal value, then c_1 must be smaller than the optimal value.

Furthermore, the analysis above is based on the optimal solution at $c_1 = 0.146$. It is worth noting that for the other optimal solution at $c_1 = 0.854$, same behaviour regarding the impact of the coupling ratios on the 3-dB bandwidth and extinction ratio is expected.

4 CONCLUSIONS

A theoretical study of all-fibre comb filter with narrow bandwidth based on a dual-pass Mach-Zehnder interferometer is presented. The condition for a lossless comb filter with narrow bandwidth is newly derived. The coupling ratios of the two couplers must be equal for achieving a lossless comb filter. Additionally, the condition for achieving a maximum extinction ratio is found to be $c_1 = c_2 = 0.146$, or 0.854. The proposed comb filter has a 3-dB bandwidth that is 27.3% smaller than that of the standard MZI. The bandwidth and the extinction ratio can be also tailored by using variable coupling ratio couplers. Narrow bandwidth with high extinction ratio could be achieved by appropriately selecting the values of the coupling ratios. This property is extremely useful for applications in reconfigurable photonic filtering, photonic signal processing, and multiwavelength fibre lasers.

ACKNOWLEDGEMENTS

This research was funded in part by the Natural Science and Engineering Research Council of Canada (NSERC) and Wilfrid Laurier University.

REFERENCES

Chen, P., Liang, X., Ma, J., Zhang, X. (2024), "Research and fabrication of the chirped Moiré fiber Bragg grating with tunable channels based on temperature control," *J. Lightw. Technol.* **42**(10), 3852-3861.

Ramírez-Meléndez, G., Bello-Jiménez, M., Pottiez, O., Andrés, M.V. (2017), "Improved all-fiber acousto-optic tunable bandpass filter," *IEEE Photon. Technol. Lett.*, **29**(12), 1015-1018.

Zhou, G., Kumar, R., et al. (2018), "A simple all-fiber comb filter based on the combined effect of multimode interference and Mach-Zehnder interferometer," *Sci. Rep.* **8**(1), 11803.

Jung, J., Lee, Y.W. (2017), "Continuously tunable polarization-independent zeroth-order fiber comb filter based on polarization-diversity loop structure," *Appl. Phys. B.*, **123**(4), 106.

Jung, J., Lee, Y.W. (2024), "Wavelength-tunable first-order narrowband fiber comb filter incorporating all-quarter-wave polarization transformation," *IEEE Photon. J.*, **16**(3), 7101007.

Zhu, Y., Cui., Z., Sun, X., Shirahata, T., Jin, L., Yamashita, S., Set, S.Y. (2020), "Fiber-based dynamically tunable Lyot filter for dual-wavelength and tunable single-wavelength mode-locking of fiber lasers," *Opt. Express*, **28**(19), 27250-27257.

Han, M., Li, X., Zhuang, S., Han, H., Liu, J., Yang, Z. (2018), "Tunable and channel spacing precisely controlled comb filters based on the fused taper technology," *Opt. Express*, **26**(1), 265-272.

Wei., L., Xu, X., Khattak, A., Henley, B. (2021), "Continuously tunable comb filter based on a highbirefringence fiber loop mirror with a polarization controller," *J. Lightw. Technol.* **39**(14), 4800-4808.

Han, Y., Liu, B., Wu, Y., Mao, Y., Zhao, L., Sun, T., Nan, T., Wang, J., Tang, R (2020), "Fiber sensor based on Fabry Perot/Mach-Zehnder hybrid interferometer for transverse load and temperature," *Microw. Opt. Technol. Lett.* **63**, 679-684.

Liu, M., Tang, M., Cao, M., Mi, Y., Guan, P., Ren, W., Ren, G. (2021), "All-fiber mode selective comb filter based on Mach–Zehnder interferometer," *Opt. Commun.*, **492**, 126964.

Cheng, W., Guo, C., Wang, J., Shi, S., Chen, Y., Wang, P., Niu, H., Hu, G., Cui, Y., Yun, B. (2024), "Flexible and reconfigurable integrated optical filter based on tunable optical coupler cascaded with coupled resonator optical waveguide," *Opt. Express*, **32**(14), 24058-24071.

Marrujo-García, S., Herrera-Piad, L.A., Hernandez-Romano, I., MayArrioja, D.A., Minkovich, V.P., Torres-Cisneros, M. (2021), "Narrow spectral linewidth and tunable erbium-doped fiber ring laser using a MZI based on CHCF," *Opt. Fiber Technol.*, **67**, 102739.

Liu, L., Chen, C., Hu, C., Zhao, P. (2024), "Narrow passband tunable optical filter based on silicon high-Q rings assisted MZI structure," *J. Lightw. Technol.* **42**(6), 2049-2056.

Jiang, X., Wu, J., Yang, Y., et al. (2016), "Wavelength and bandwidth-tunable silicon comb filter based on Sagnac loop mirrors with Mach-Zehnder interferometer couplers," *Opt. Express* **24**(3), 2183-2188.

Luo, Z., Cao, W., Luo, A., Xu, W. (2012), "Polarization-independent, multifunctional all-Fiber comb filter using variable ratio coupler-based Mach–Zehnder Interferometer," *J. Lightw. Technol.* **30**(12), 1857-1862.

Wei., L., Tatel, G. (2019), "Wavelength continuously tunable all-fiber flat-top comb filter based on a dual-pass Mach–Zehnder interferometer," *J. Lightw. Technol.* **37**(15), 3740-3749.